^{1}H and ^{2}H NMR relaxation study on the phase transitions of $(NH_4)_3H(SO_4)_2$ and $(ND_4)_3D(SO_4)_2$ single crystals

2006 J. Phys.: Condens. Matter 18 6759

(http://iopscience.iop.org/0953-8984/18/29/015)

INSTITUTE OF PHYSICS PUBLISHING JOURNAL OF PHYSICS: CONDENSED MATTER

J. Phys.: Condens. Matter **18** (2006) 6759–6768 doi:10.1088/0953-8984/18/29/015

^{1}H and ^{2}H NMR relaxation study on the phase transitions of $(NH_4)_3H(SO_4)_2$ and $(ND_4)_3D(SO_4)_2$ single crystals

Ae Ran Lim[1,3] **and Se-Young Jeong**[2]

[1] Department of Science Education, Jeonju University, Jeonju 560-759, Chonbuk, Korea
[2] School of Nanoscience and Technology, Pusan National University, Pusan 609-735, Korea

E-mail: aeranlim@hanmail.net and arlim@jj.ac.kr

Received 25 January 2006, in final form 14 June 2006
Published 3 July 2006
Online at stacks.iop.org/JPhysCM/18/6759

Abstract

T_1, $T_{1\rho}$ and T_2 for the ^{1}H and ^{2}H nuclei in $(NH_4)_3H(SO_4)_2$ and $(ND_4)_3D(SO_4)_2$ single crystals grown using the slow evaporation method were measured for phases I, II, III, IV and V. The ^{1}H T_1, $T_{1\rho}$, and T_2 values were found to exhibit different trends in phases II and III: T_1, $T_{1\rho}$ and T_2 for ^{1}H do not change significantly near the phase transition at 265 K, whereas near 413 K they change discontinuously. We conclude that the NH_4^+ and $H(SO_4)_2^-$ ions do not play an important role in the III–II phase transition, but do play important roles in the II–I phase transition. The liquid-like nature of the ^{1}H $T_{1\rho}$ and T_2 above 413 K is indicative of the destruction and reconstruction of hydrogen bonds. Moreover, the phase transitions of the $(NH_4)_3H(SO_4)_2$ crystal are accompanied by changes in the molecular motion of the $(NH_4)^+$ ions. The variations with temperature of the ^{2}H T_1 and T_2 of $(ND_4)_3D(SO_4)_2$ crystals are not similar to those observed for the ^{1}H T_1 and T_2. Our comparison of the results for $(NH_4)_3H(SO_4)_2$ and $(ND_4)_3D(SO_4)_2$ crystals indicates the following: the ^{1}H $T_{1\rho}$ and T_2 of the $(NH_4)^+$ and $H(SO_4)_2^-$ ions above T_{C1} are characteristic of fast, liquid-like motion, which is not the case for $(ND_4)_3D(SO_4)_2$; and the ^{2}H T_1 of $D(SO_4)_2^-$ in $(ND_4)_3D(SO_4)_2$ is longer than the ^{2}H T_1 of $(ND_4)^+$ in contrast to the results for $(NH_4)_3H(SO_4)_2$ crystals.

1. Introduction

Compounds of the type $Me_3H(XO_4)_2$ (Me = Na, K, Rb, Cs, NH_4; X = S, Se) that exhibit a dynamic network of hydrogen bonds in a high temperature superionic phase are of great scientific interest because of their phase transitions and proton transport mechanisms [1]. Because of their high proton conductivity at low and intermediate temperatures, these

[3] Author to whom any correspondence should be addressed.

compounds might have practical applications in devices such as hydrogen sensors [2]. Proton conduction occurs in several types of materials, including many hydrogen-bonded systems. $(NH_4)_3H(SO_4)_2$ and its deuterated analogue $(ND_4)_3D(SO_4)_2$ belong to the well-known family of superionic proton conductors with the general formula $Me_3H(XO_4)_2$ [3, 4]. The crystals of the $Me_3H(XO_4)_2$ family undergo a superionic phase transition in their high temperature phases. However, $(NH_4)_3H(SO_4)_2$ and $(ND_4)_3D(SO_4)_2$ crystals exhibit phase transitions not only at high temperatures but also below room temperature. These crystals are of special interest because of this diversity of phase transitions. It is known that $(NH_4)_3H(SO_4)_2$ undergoes five phase transitions, at 413, 265, 139, 133 and 63 K, and has six phases [5, 6], denoted I, II, III, IV, V and VI in order of decreasing temperature. Phase I is a superionic conductor, phase II is ferroelastic [7], phases III and V are antiferroelectric, phase IV is incommensurate and phase VI is ferroelectric. $(ND_4)_3D(SO_4)_2$ is known to undergo five phase transitions at about 395, 264, 249, 209 and 173 K with six phases [8, 9]. These phases are denoted I, II, III, VI, III′ and VII in order of decreasing temperature. This crystal is a superionic conductor in phase I, and is ferroelectric in phases VI and VII. The temperatures of the phase transitions between phases VII, III′, VI, III, II and I of $(ND_4)_3D(SO_4)_2$ are denoted T_{C5}, T_{C4}, T_{C3}, T_{C2} and T_{C1}, respectively. It has recently been reported that the $(NH_4)_3H(SO_4)_2$ and $(ND_4)_3D(SO_4)_2$ crystals undergo additional phase transitions at 463 and 413 K, respectively [10, 11]. The proton transfer dynamics in the hydrogen bond for the crystals of the $Me_3H(XO_4)_2$ family have previously been reported using inelastic neutron scattering, infrared and Raman spectra [1]. In addition, the role of different H-bonds in phases II, III, IV and V of $(NH_4)_3H(SO_4)_2$ has been studied by x-ray diffraction and ^{1}H solid-state magic angle spinning (MAS) nuclear magnetic resonance (NMR) [12]. Although the physical properties of the two crystals have previously been reported, no investigation with NMR for the mechanisms of their phase transitions has yet been conducted.

The relationship between the dynamic transfer of hydrogen atoms and structural phase transitions has been a subject of keen interest. In this connection, the protons and deuterons of $(NH_4)_3H(SO_4)_2$ and $(ND_4)_3D(SO_4)_2$ single crystals are particularly worthy of study. In an attempt to elucidate the mechanisms of the successive phase transitions of $(NH_4)_3H(SO_4)_2$ and $(ND_4)_3D(SO_4)_2$ single crystals, we characterized the molecular motions of the NH_4^+ and $H(SO_4)_2^-$ groups in these crystals by measuring the spin–lattice relaxation time, T_1, and the spin–spin relaxation time, T_2. In this paper, the temperature dependences of T_1 and T_2 for the ^{1}H and ^{2}H nuclei in $(NH_4)_3H(SO_4)_2$ and $(ND_4)_3D(SO_4)_2$ single crystals were determined in order to elucidate the mechanisms of their structural phase transitions, with particular emphasis on the role within those mechanisms of hydrogen bonding. The NMR characteristics of the ^{1}H and ^{2}H nuclei in $(NH_4)_3H(SO_4)_2$ and $(ND_4)_3D(SO_4)_2$ crystals have been observed, and we use these results to discuss the crystals' phase transitions and molecular motion.

2. Crystal structure

The $(NH_4)_3H(SO_4)_2$ crystal is monoclinic at room temperature [4, 13, 14]. The crystal structure is shown in figure 1. There are 12 ammonium ions and 8 sulfate ions in the unit cell, in which each pair of neighbouring sulfate ions is linked by one hydrogen bond of type O–H$\cdots$O, i.e. there are four hydrogen bonds of this type. The sulfate ion forms a slightly distorted tetrahedron. The NH_4^+ tetrahedra are nearly regular, and linked to SO_4^{2-} ions by hydrogen bonds [15]. The crystal structure of phase I is trigonal with space group $R\bar{3}m$ or $R\bar{3}c$ [16]. The structure of $(NH_4)_3H(SO_4)_2$ is known to be monoclinic (space group $C2/c$ or $A2$) in phase II, monoclinic (space group $P2/n$ or Pn) in phase III and monoclinic (space group $C2$) in phase V [17–19].

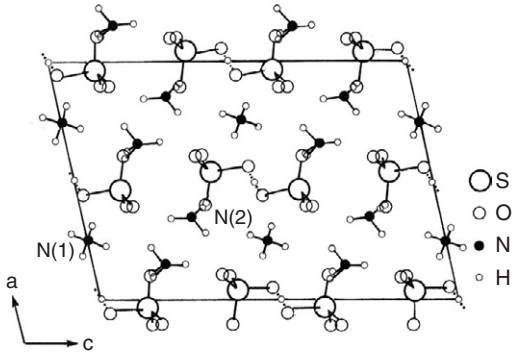

Figure 1. The structure of a $(NH_4)_3H(SO_4)_2$ single crystal projected along the *b*-axis. Dotted lines indicate hydrogen bonds of type O–H$\cdots$O. Hydrogen bonds of type N–H$\cdots$O are not shown because of their complexity.

The $(ND_4)_3D(SO_4)_2$ crystal is monoclinic at room temperature [20], and the crystal structure of phase I belongs to trigonal $R\bar{3}m$ [21]. The structure of $(ND_4)_3D(SO_4)_2$ is reported to be monoclinic (space group $C2/c$) in phase II, triclinic (space group $P1$) in phase VI and monoclinic (space group $P2$) in phase III$'$ [22, 23]. The crystal structure of $(ND_4)_3D(SO_4)_2$ is similar to that of the $(NH_4)_3H(SO_4)_2$ crystal, which is shown in figure 1.

3. Experimental method

The $(NH_4)_3H(SO_4)_2$ single crystals were grown using slow evaporation from an aqueous solution containing $(NH_4)_2SO_4$ and H_2SO_4. The $(ND_4)_3D(SO_4)_2$ single crystals were grown using slow evaporation from an aqueous D_2O solution containing $(NH_4)_2SO_4$ and D_2SO_4. The crystals were found to be pseudo-hexagonal plates with predominant *c*-plane (001) faces. The crystals were colourless and transparent with hexagonal shapes.

The NMR signals of the ^{1}H and ^{2}H nuclei in the $(NH_4)_3H(SO_4)_2$ and $(ND_4)_3D(SO_4)_2$ single crystals were measured using the Varian 200 FT NMR and Bruker 400 FT NMR spectrometers at the Korea Basic Science Institute. The static magnetic field and the central radio frequency for the ^{1}H nucleus were the 4.7 T spectrometer and $\omega_0/2\pi = 200$ MHz. In the case of the ^{2}H nucleus, the static magnetic field was for the 9.4 T spectrometer and the central radio frequency was set at $\omega_0/2\pi = 61.40$ MHz. The ^{1}H and ^{2}H experiments were performed using a $\pi - t - \pi/2$ pulse sequence for the T_1 measurements, a spin-locking sequence $\pi - B_1(t)$ with $B_1 = 5$ kHz for the $T_{1\rho}$ measurements, and T_2 was measured with the solid echo sequence. The nuclear magnetizations $S(t)$ of the ^{1}H and ^{2}H nuclei at time t after the π pulse were determined from the inversion recovery sequence following the pulse. The widths of the π pulses were 3 μs and 2.5 μs for ^{1}H and ^{2}H, respectively. The NMR measurements were obtained in the temperature range 160–430 K. The sample temperatures were maintained at a constant value by controlling the helium gas flow and the heater current, giving an accuracy of ± 0.5 K.

4. Experimental results and analysis

To determine the phase transition temperatures of the $(NH_4)_3H(SO_4)_2$ and $(ND_4)_3D(SO_4)_2$ crystals, differential scanning calorimetry (DSC) was carried out on the crystals using a Dupont

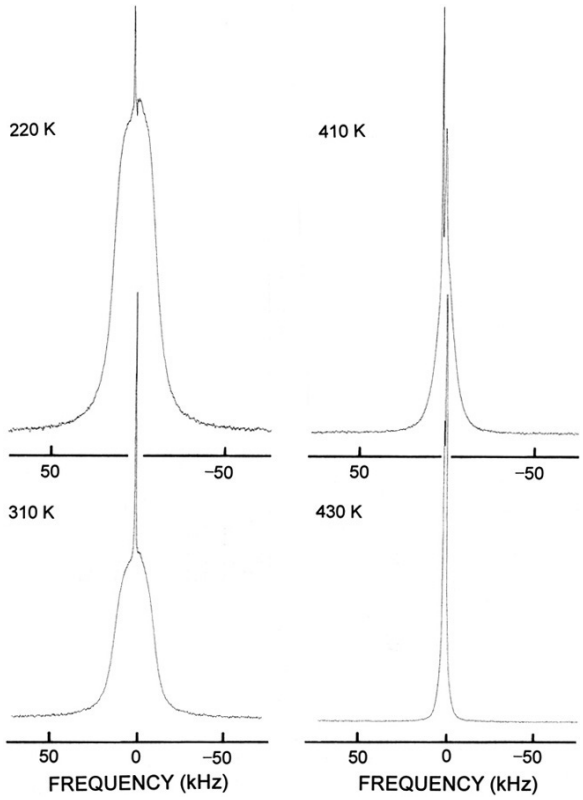

Figure 2. The 'ammonium' and 'hydrogen-bond' proton NMR spectra for a $(NH_4)_3H(SO_4)_2$ crystal as a function of temperature.

2010 DSC instrument. The measurements were performed at a heating rate of 10 K min^{-1}. The phase transition temperatures of $(NH_4)_3H(SO_4)_2$ and $(ND_4)_3D(SO_4)_2$ obtained from the DSC measurements are consistent with previously reported results. However, phase transitions at 463 K for $(NH_4)_3H(SO_4)_2$ and 413 K for $(ND_4)_3D(SO_4)_2$ were not observed.

4.1. ^1H spin–lattice relaxation and spin–spin relaxation times in $(NH_4)_3H(SO_4)_2$

The NMR spectrum for the ^1H nuclei in a $(NH_4)_3H(SO_4)_2$ crystal was measured as a function of temperature. There are two kinds of protons in $(NH_4)_3H(SO_4)_2$, the 'ammonium' protons for which relaxation is mainly determined by hindered rotation of the NH_4 groups, and the 'hydrogen-bond' protons for which relaxation is mainly determined by the motion of the hydrogen in the hydrogen sulfate ion. In our results, the proton signals due to the ammonium and hydrogen-bond protons overlap, as shown in figure 2. Here, the crystal orientation with respect to magnetic field was along the *c*-axis. The broad and narrow lines shown in figure 2 are due to the ammonium and hydrogen-bond protons, respectively. The line width of the signal due to the ammonium protons is very broad at room temperature, whereas the line width of the signal due to the hydrogen-bond protons is very narrow. The line width of the signal due to the ammonium protons abruptly narrows near 410 K, which indicates that the ammonium protons play an important role in this phase transition.

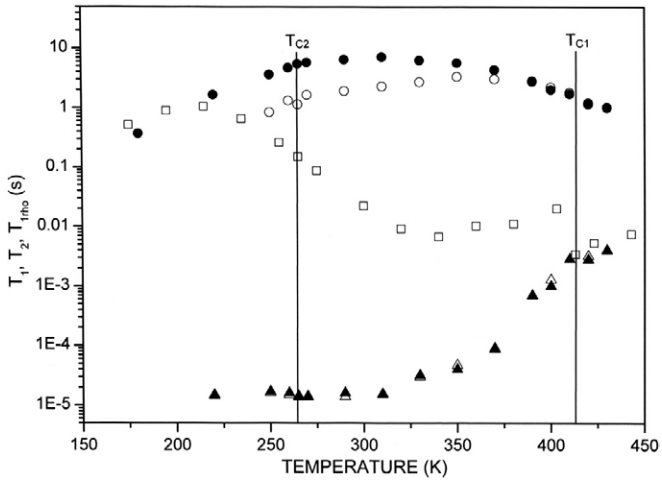

Figure 3. Temperature dependences of the spin–lattice relaxation time, T_1, and the spin–spin relaxation time, T_2, in the laboratory frame, the spin–spin relaxation time in the rotating frame, $T_{1\rho}$ of ^{1}H nuclei in a $(NH_4)_3H(SO_4)_2$ crystal (○: hydrogen-bond ^{1}H T_1; ●: ammonium ^{1}H T_1; □: ^{1}H $T_{1\rho}$; Δ: hydrogen-bond ^{1}H T_2; ▲: ammonium ^{1}H T_2).

The variations with temperature of T_1, $T_{1\rho}$ and T_2 for protons in $(NH_4)_3H(SO_4)_2$ crystals are shown in figure 3. The T_1 for the ammonium and hydrogen bond protons do not change significantly at T_{C1} and T_{C2}. However, the T_1 of the ammonium protons is longer than that of the hydrogen-bond protons at low temperatures; at high temperatures they have the same value. In the low-temperature phase, T_1 differs from $T_{1\rho}$, which is in turn different from T_2. In phases II and III, the proton NMR free induction decay is rapid, indicative of a rigid lattice. T_1 is more or less continuous at T_{C2} (=265 K), which suggests that the crystal lattice does not change very much in this transition. The variation of the T_1 of $(NH_4)^+$ in phases II and III is larger than that of the T_1 of $H(SO_4)_2^-$, which indicates that the ammonium protons are more involved in this phase transition. There is, however, a sharp decrease in $T_{1\rho}$, which can be ascribed to the onset of the slow translational diffusion of the protons. In phase II, it is apparent that T_1 and $T_{1\rho}$ are not governed by the same mechanism. T_1 in phase II is determined by fast $H(SO_4)_2^-$ molecular motion and slow $(NH_4)^+$ rotational reorientations, whereas $T_{1\rho}$ is determined by slow proton translational diffusion. The decrease in $T_{1\rho}$ in phase II can be ascribed to the onset of the slow translational diffusion of protons, whereas the change in $T_{1\rho}$ is generated by the onset of the slow translational jumps of protons, which produces a minimum in $T_{1\rho}$. The minimum in $T_{1\rho}$ occurs at 340 K, which for $\omega_1\tau_C = 1$ is at 10 ms. This feature of $T_{1\rho}$ indicates that distinct molecular motion is present. In phase II below 413 K, the form of the proton $T_{1\rho}$ versus temperature curves leads us to believe that the relaxation process is affected by molecular motion. The $T_{1\rho}$ for ^{1}H in $(NH_4)_2H(SO_4)_2$ crystals used here has a well-defined minimum in the Bloembergen–Purcell–Pound (BPP) theory [24, 25].

The values of $T_{1\rho}$ can be related to the corresponding values of the rotational correlation time, τ_C, which is the length of time a molecule remains in a given state before the molecule reorients. As such, τ_C is a direct measure of the rate of motion. For the spin–lattice relaxation time in a rotating frame, the experimental value of $T_{1\rho}$ can be expressed in terms of the correlation time τ_C for molecular motion by using the following equation:

$$T_{1\rho}^{-1} = (N/20)(\gamma_H\gamma_N\hbar/r^3)^2[4A + B + 3C + 6D + 6E], \tag{1}$$

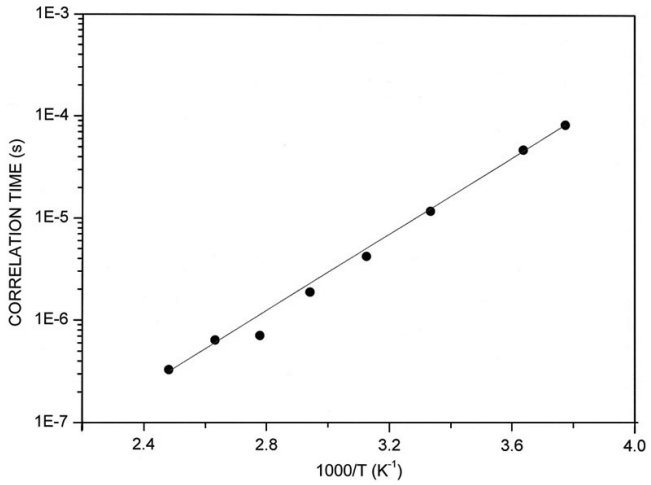

Figure 4. Arrhenius plot of the natural logarithm of the correlation times as a function of the inverse temperature.

where

$$A = \tau_C/[1 + \omega_1^2\tau_C^2],$$
$$B = \tau_C/[1 + (\omega_H - \omega_N)^2\tau_C^2],$$
$$C = \tau_C/[1 + \omega_N^2\tau_C^2],$$
$$D = \tau_C/[1 + (\omega_H + \omega_N)^2\tau_C^2],$$
$$E = \tau_C/[1 + \omega_H^2\tau_C^2].$$

Here, γ_H and γ_N are the gyromagnetic ratios for the ^{1}H and ^{14}N nuclei, respectively, N is the number of directly bound protons, r is the H–N distance, $\hbar = h/2\pi$ (where $\hbar$ is the Planck constant), ω_H and ω_N are the Larmor frequencies of ^{1}H and ^{14}N, respectively, and ω_1 is the spin-lock field. In the present study, the MATHEMATICA package was used to obtain the correlation time by the variations of $T_{1\rho}$ as a function of the temperature. Since the experimental results were obtained using a spin-locking field ($\omega_1 = 83.33 \times 2\pi \times 10^3$ rad s^{-1}), the minimum of the correlation time τ_C occurred at 1.91 μs, considering $\omega_1\tau_C = 1$. The size of the minimum was determined from the magnitude of the second moment modulated by variation of the H–N dipolar interaction. We sensitively controlled the minima in the $T_{1\rho}$ temperature variations and the slopes around the minima. From this result, the value of $(\gamma_H\gamma_N\hbar/r^3)^2$ in equation (1) is obtained, and we calculated the temperature dependence of the τ_C by using the value of $(\gamma_H\gamma_N\hbar/r^3)^2$, and the result is shown in figure 4. The temperature dependence can be obtained by assuming a simple Arrhenius expression:

$$\tau_C = \tau_0 \exp(E_a/RT). \tag{2}$$

where E_a is the activation energy for molecular motion, R is the gas constant, and τ_C is the correlation time $T \to \infty$. Thus, a plot of the natural logarithm of the correlation time as a function of the inverse temperature is linear with a slope that is directly related to the activation energy for motion. The activation energy for the molecular motion in phase II was determined to be 35.8 kJ mol^{-1}.

T_2 abruptly increases in phase I, the fast-ion conductor phase. This situation is analogous to that for $CsHSO_4$ [26]. Above $T_{C1} = 413$ K, T_2 becomes liquid-like (i.e. of the order of several

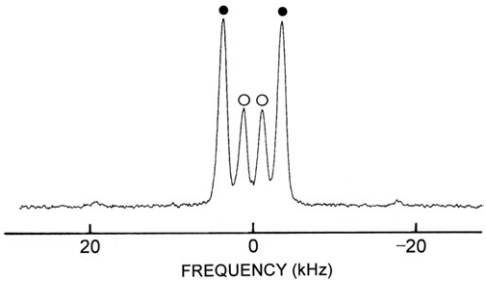

Figure 5. The 'ammonium' and 'hydrogen-bond' deuteron NMR spectra of a $(ND_4)_3D(SO_4)_2$ crystal (●: ammonium ^2H signals; ○: hydrogen-bond ^2H signals).

milliseconds), which indicates the presence of translational diffusion in addition to molecular 'rotation'. The changes in T_1, $T_{1\rho}$ and T_2 at $T_{C1} = 413$ K suggest the occurrence of a structural phase transition. The liquid-like values at high temperatures indicate that the phase above T_{C1} is superionic. As the temperature increases, ω_c (reorientation) speeds up, causing a narrowing of the proton NMR line width and, as a result, T_2 increases. This increase in T_2 is due to the rapid motion of the protons in the $(NH_4)^+$ and $H(SO_4)_2^-$ ions, giving rise to different, well-defined 'orientations'. From the temperature dependences of T_1 and T_2, we conclude that at temperatures below those of the superionic phase, $\omega_{dip} \ll \omega_c$ (reorientation) $< \omega_0$. Here ω_{dip} is the proton Larmor frequency in the local dipolar field (i.e. the dipolar width of the proton line expressed in frequency units), ω_c (reorientation) is the frequency of the rotational motions of the $(NH_4)^+$ and $H(SO_4)_2^-$ groups between the different equilibrium orientations, ω_c (translation) is the frequency of the motions of the protons between different sites due to translational diffusion and ω_0 is the Larmor frequency in the external magnetic field.

4.2. ^2D spin–lattice relaxation and spin–spin relaxation times in $(ND_4)_3D(SO_4)_2$

There are two kinds of deuteron in the unit cell of $(ND_4)_3D(SO_4)_2$ crystals, 'ammonium' deuterons and 'hydrogen-bond' deuterons, so the ^2H ($I = 1$) NMR spectrum is expected to consist of four lines. The signals due to the 'ammonium' and 'hydrogen-bond' deuterons are shown in figure 5. The stronger and weaker signals are due to the $(ND_4)^+$ and $D(SO_4)_2^-$ nuclei, respectively. The two central resonance lines are of low intensity, whereas the side resonance lines are of high intensity. The splitting of the ^2H resonance lines for the two kinds of deuterons was found to change slightly with increases in temperature, i.e. the spacing between the resonance lines decreases, as shown in figure 6. The spacing between the resonance lines with low intensity is nearly constant with increasing temperature, whereas the spacing between the resonance lines with high intensity decreases abruptly with increasing temperature. This is because the quadrupole parameter of ^2H in $(ND_4)^+$ is larger than that of ^2H in $D(SO_4)_2^-$. The change in the splitting of the ammonium ^2H resonance line at the phase transition temperature of 264 K indicates that the electric field gradient (EFG) at the ammonium sites changes with temperature, and thus that the deuterons' neighbouring atoms are displaced in this phase transition. We conclude that the ammonium groups play an important role in the II–III phase transition. This is consistent with the x-ray diffraction finding by Dominiak *et al* [1] that the ammonium tetrahedron does significantly change its position.

The same overall trend was also observed for the ^2H relaxation time in the deuterated compound; the spin–lattice relaxation and spin–spin relaxation times for the four lines of ^2H in $(ND_4)_3D(SO_4)_2$ crystals were measured as a function of temperature. The recovery traces

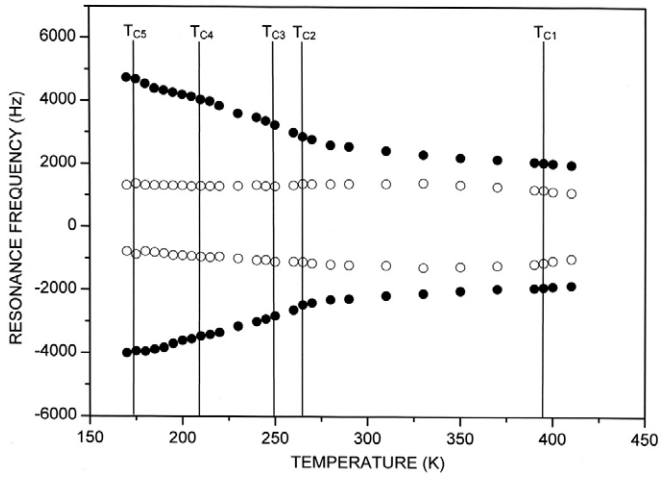

Figure 6. Splitting of the ^{2}H resonance line as a function of temperature for a $(ND_4)_3D(SO_4)_2$ crystal.

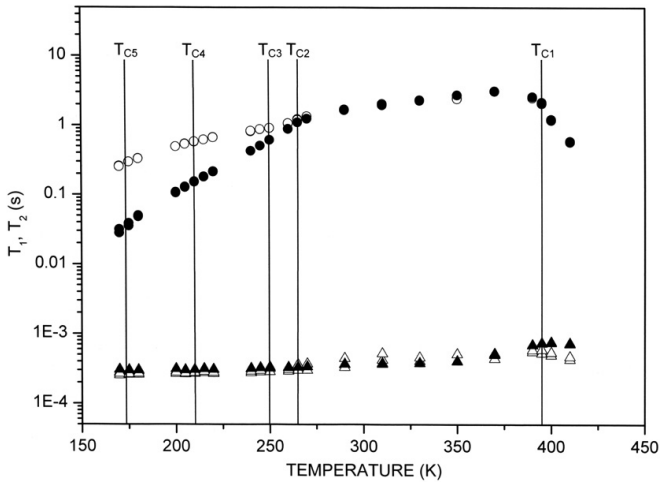

Figure 7. Temperature dependences of the spin–lattice relaxation time, T_1, and the spin–spin relaxation time, T_2, of ^{2}H nuclei in a $(ND_4)_3D(SO_4)_2$ crystal (○: hydrogen-bond ^{2}H T_1; ●: ammonium ^{2}H T_1; △: hydrogen-bond ^{2}H T_2; ▲: ammonium ^{2}H T_2).

for the four resonance lines of ^{2}H can be represented with a single exponential function. The ^{2}H relaxation times in $(ND_4)_3D(SO_4)_2$ crystals are displayed in figure 7. The values of T_1 for the 'ammonium' and 'hydrogen-bond' deuterons are different below T_{C2} (=264 K); however, T_1 for the two kinds of deuterons indicate that the same fast motion is occurring in both cases. The values of T_1 for the two resonance lines above T_{C2} (=264 K) are also very similar, and are the same within experimental error. The relaxation time for the ^{2}H nuclei in $(ND_4)^+$ undergoes a significant change above 264 K. The decrease in T_1 near T_{C1} (=395 K) is due to a structural phase transition. The ^{2}H T_1 of $(ND_4)^+$ abruptly changes at T_{C1} and T_{C2}, which indicates that the 'ammonium' deuterons play an important role in these phase transitions.

The phase transitions at 173, 209 and 249 K do not appear to affect the ^{2}H T_1 NMR results. The variation in ^{2}H T_1 with increasing temperature is larger than the variation of ^{1}H T_1.

In addition, the spin–spin relaxation time, T_2, was found to depend on temperature. As shown in figure 7, T_1 abruptly decreases with increasing temperature, whereas T_2 slowly increases. The ^{2}H T_1 of $(ND_4)^+$ and $D(SO_4)_2^-$ in $(ND_4)_2D(SO_4)_2$ rapidly decrease above T_C on heating, and reach a value of $T_1 = 580$ ms at 410 K. The temperature dependences of the relaxation times in the protonated and deuterated compounds are not the same.

5. Discussion and conclusion

The spin–lattice relaxation time in the laboratory frame, T_1, the spin–lattice relaxation time in the rotating frame, $T_{1\rho}$, and the spin–spin relaxation time, T_2, of the ^{1}H and ^{2}H nuclei in $(NH_4)_3H(SO_4)_2$ and $(ND_4)_3D(SO_4)_2$ single crystals were investigated with NMR spectrometry. These NMR observations provide a consistent description of the dynamics of the ^{1}H and ^{2}H nuclei in this material. The ^{1}H T_1, $T_{1\rho}$ and T_2 for $(NH_4)^+$ and $H(SO_4)_2^-$ in $(NH_4)_3H(SO_4)_2$ do not change significantly near the phase transition at 265 K, whereas they change discontinuously near 413 K. We conclude that the $(NH_4)^+$ and $H(SO_4)_2^-$ ions do not play important roles in the III–II phase transition, but do play important roles in the II–I phase transition. The appearance of liquid-like proton $T_{1\rho}$ and T_2 above $T_{C1} = 413$ K indicates that a transition to a superionic phase takes place at this temperature in $(NH_4)_3H(SO_4)_2$ crystals. The mechanism of fast proton conduction is connected with the rupture of the weak part of the O–H$\cdots$O bond and the formation of a new H-bond in $H(SO_4)_2^-$; the ^{1}H $T_{1\rho}$ and T_2 of $(NH_4)_3H(SO_4)_2$ crystals are liquid-like, which is indicative of the destruction and reconstruction of hydrogen bonds. This behaviour is expected for most hopping-type ionic conductors, and can be attributed to interactions between the mobile ions and the neighbouring group ions within the crystal. Moreover, the phase transitions in the $(NH_4)_3H(SO_4)_2$ crystal are accompanied by changes in the molecular motion of the $(NH_4)^+$ ions. On the other hand, the ^{2}H T_1 values of $(ND_4)^+$ and $D(SO_4)_2^-$ in $(ND_4)_3D(SO_4)_2$ crystals are different below 264 K but the same above this temperature. The variations of the ^{2}H T_1 with temperature were found to be different from those observed for the ^{1}H T_1. Below T_{C2}, ^{1}H T_1 of $(NH_4)^+$ in $(NH_4)_3H(SO_4)_2$ crystals is longer than the ^{1}H T_1 of $H(SO_4)_2^-$, whereas the ^{2}H T_1 of $D(SO_4)_2^-$ in $(ND_4)_3D(SO_4)_2$ is longer than the ^{2}H T_1 of $(ND_4)^+$. We found considerable differences between the properties of the undeuterated and deuterated isomorphs. The conclusions of our comparison of the results for $(NH_4)_3H(SO_4)_2$ and $(ND_4)_3D(SO_4)_2$ crystals can be summarized as follows: (1) the ^{1}H $T_{1\rho}$ and T_2 of the $(NH_4)^+$ and $H(SO_4)_2^-$ ions above T_{C1} are characteristic of fast, liquid-like motion, which is not the case for $(ND_4)_3D(SO_4)_2$; and (2) the ^{2}H T_1 of $D(SO_4)_2^-$ in $(ND_4)_3D(SO_4)_2$ is longer than the ^{2}H T_1 of $(ND_4)^+$ in contrast to the results for $(NH_4)_3H(SO_4)_2$ crystals. The present results indicate that for both crystal types, the main contribution to the phase transitions comes from molecular motion of ammonium ions and the motion of protons in hydrogen-bonded groups. The present NMR study of single crystals has provided new information on the roles of 'ammonium' and 'hydrogen-bond' protons, information that cannot be obtained from powder data.

Acknowledgment

This work was supported by a Korea Research Foundation Grant (KRF-2004-015-C00148).

References

[1] Fillaux F, Lautie A, Tomkinson J and Kearley G J 1991 *Chem. Phys.* **154** 135
[2] Ponomareva V G, Merinov B V and Dolbinina V V 2001 *Solid State Ion.* **145** 205

[3] Sooryanarayana K and Guru Row T N 1996 *Phase Transit.* **58** 263
[4] Kamoun M, Lautie A, Romair F, Limage M H and Novak A 1988 *Spectrosc. Acta* A **44** 471
[5] Gesi K 1976 *Phys. Status Solidi* a **33** 479
[6] Gesi K 1977 *J. Phys. Soc. Japan* **43** 1941
[7] Fujimoto M and Sinha B V 1983 *Ferroelectrics* **46** 227
[8] Osaka T, Makita Y and Gesi K 1977 *J. Phys. Soc. Japan* **43** 933
[9] Osaka T, Makita Y and Gesi K 1980 *J. Phys. Soc. Japan* **49** 593
[10] Fukami T, Ninomiya H and Chen R H 1997 *Solid State Ion.* **98** 105
[11] Fukami T, Horiuchi K and Chen R H 2000 *Solid State Ion.* **131** 275
[12] Dominiak P M, Herold J, Kolodziejski W and Wozniak K 2003 *Inorg. Chem.* **42** 1590
[13] Suzuki S and Makita Y 1978 *Acta Crystallogr.* B **34** 732
[14] Smirnov L S, Baranov A I, Shuvalov L A, Sarga L B, Natkaniec I and Waplak S 2001 *Phys. Solid State* **43** 117
[15] Leclaire P A, Ledesert M, Monier J C, Daoud A and Damak M 1985 *Acta Crystallogr.* B **41** 209
[16] Fukami T, Horiuchi K, Nakasone K and Furukawa K 1996 *Japan. J. Appl. Phys.* **35** 2253
[17] Tamura I, Noda Y and Morii Y 1999 *J. Phys. Chem. Solid* **60** 1411
[18] Kamoun M, Ben Ghozlen M H and Daoud A 1987 *Phase Transit.* **9** 247
[19] Chen R H, Wang L M and Yang S C 1992 *Phase Transit.* **37** 141
[20] Tanaka M and Shiozaki Y 1981 *Acta Crystallogr.* B **37** 1171
[21] Fukami T, Horiuchi K and Chen R H 2000 *Solid State Ion.* **131** 275
[22] Tanaka M and Shiozaki Y 1986 *Acta Crystallogr.* C **42** 776
[23] Kasahara M and Yagi T 2002 *Ferroelectrics* **266** 131
[24] Bloembergen N, Purcell E M and Pound R V 1948 *Phys. Rev.* **73** 679
[25] Harris R K 1986 *Nuclear Magnetic Resonance Spectroscopy* (New York: Longman)
[26] Damyanovich A, Pintar M M, Blinc R and Slak J 1997 *Phys. Rev.* B **56** 7942